ACS APPLIED MATERIALS & INTERFACES

Letter

www.acsami.org

Efficiency Enhancement in Polymer Light-Emitting Diodes via Embedded Indium–Tin–Oxide Nanorods

Husan-De Li,[†] Chia-Shuo Hsu,[†] Fu-Min Zhan,[†] and Yu-Chiang Chao*[,†,‡]

[†]Department of Physics and [‡]Center for Nanotechnology, Chung Yuan Christian University, Chung-Li 32023, Taiwan

Supporting Information

ABSTRACT: Indium–tin–oxide (ITO) nanorods were fabricated in 10 min from commercially available ITO substrate using wet chemical etching method. The optical properties of the ITO nanorods were investigated using transmission spectroscopy and dark-field optical microscopy. The transmittance and light-scattering characteristics of the ITO nanorods were better than those of ITO film. The ITO nanorod layer was further used as a transparent anode in polymer light-emitting diodes (PLEDs). The brightness and current efficiency of the PLED with the ITO nanorod layer were enhanced. This performance enhancement can be attributed to the excellent optical and electrical properties of the ITO nanorod layer.

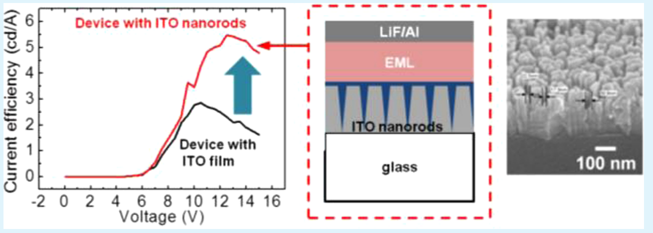

KEYWORDS: *polymer light-emitting diodes, light extraction, antireflection, light scattering*

Polymer light-emitting diodes (PLEDs) have attracted considerable attention because of their advantages such as low power consumption, light weight, and flexibility. However, the performance of PLEDs must be further optimized to ensure their possible commercialization. Conventional PLEDs have a multilayer structure consisting of glass substrate, an indium–tin–oxide (ITO) transparent electrode, a hole injection layer, emissive and transport layers, and a cathode. The refractive indices (n) of glass, ITO, and a well-known hole injection layer poly(3,4-ethylenedioxythiophene):poly(styrenesulfonate) (PEDOT:PSS) are functions of wavelength and are approximately 1.5–1.6, 1.8–2.3, and 1.5–1.7, respectively.[1−3] However, because of the large difference in their refractive indices, the generated light is confined in devices, thus resulting in low out-coupling efficiency. Approximately 80% of the photons are trapped in different waveguide modes.[4−6] Substrate waveguide mode is caused by total internal reflection in a glass substrate. To extract light from substrate waveguide mode, numerous light out-coupling techniques including patterned substrates,[7−9] high refractive index substrates,[10] and microlens arrays have been employed.[11,12] Similarly, the total internal reflection occurring in ITO/organic layers leads to an ITO/organic waveguide mode. Devices with photonic crystals,[13−15] micocavities,[16,17] and surface plasmons[18−20] have been developed to extract light from ITO/organic waveguide mode. However, only a few studies[4] have incorporated light-extraction nanostructures for ITO, which has the highest refractive index in conventional PLEDs. Moreover, most of the proposed fabrication procedures for light out-coupling nanostructures involve sophisticated and expensive fabrication technologies, such as nanoimprint and electron-beam lithography. Therefore, an easy and economical procedure must be developed for fabricating light out-coupling nanostructures with excellent light-extraction characteristics.

In this study, ITO nanorods were fabricated using wet chemical etching method, and the fabricated ITO nanorods were embedded, for the first time, in PLEDs as a light-extraction layer. ITO nanorods with approximately 30 nm diameter and 120 nm height were obtained in 10 min. The transmittance and light-scattering characteristics of the ITO nanorod layer are enhanced. The PLED with the ITO nanorod layer exhibits more brightness and higher efficiency than the reference device without ITO nanorod layer. Because of the excellent optical and electrical properties of the ITO nanorods, light was extracted from the ITO/organic waveguide mode, and maximum current efficiency was improved by 91%.

The ITO nanorods were fabricated from a commercially available ITO-coated glass substrate using wet chemical etching method (Figure 1). The substrates were submerged in phosphoric acid, and the etching process was stopped after a certain amount of time.[21] The formation of ITO nanorods under different etching times was analyzed using SEM images of the substrates, as shown in Figure 2. The original thickness of the ITO film is approximately 250 nm (Figure 2a). As the etching time increases, cracks are formed, and the gaps between the ITO nanorods increase. If the etching time is inadequate, the ITO nanorods are not completely formed. ITO nanorods suitable for this study can be achieved in 10 min, as shown in Figure 2c. The ITO nanorods are vertically oriented on a continuous ITO layer. The height and diameter of the ITO nanorods are approximately 120 and 30 nm, respectively. The

Received: February 6, 2015
Accepted: March 30, 2015
Published: April 1, 2015

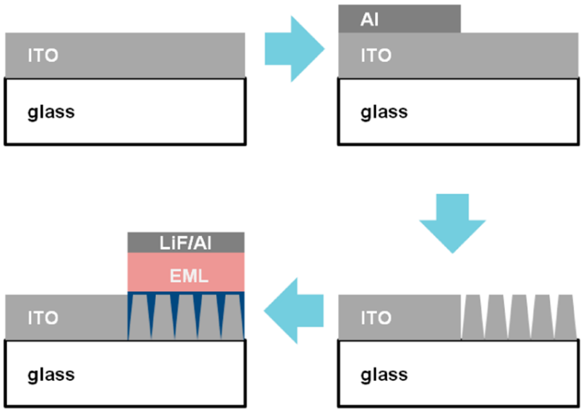

Figure 1. Fabrication procedures of ITO nanorods and polymer light-emitting diodes.

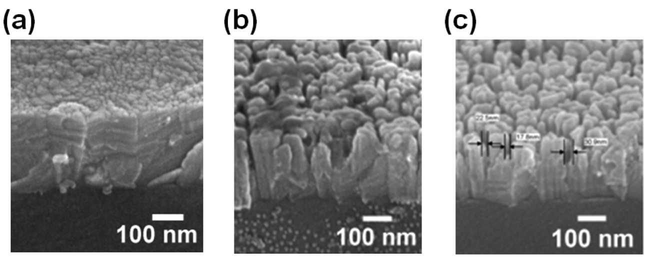

Figure 2. SEM images of ITO layers etched for (a) 0, (b) 5, and (c) 10 min.

existence of a continuous ITO layer is crucial for providing the electrical conduction path. If the etching time is extended, the ITO will be over etched, and a continuous ITO layer cannot be observed on the substrate. The resistance of an overetched ITO nanorod layer will be dramatically increased; therefore, an overetched ITO nanorod layer is not suitable for electronic devices.

Transmittance spectroscopy and dark-field microscopy were used to investigate the optical properties of the ITO nanorod layer, as shown in Figure 3. The ITO film exhibits Fabry−Pérot resonance[22] with transmission peaks at 480 and 710 nm, as shown in Figure 3a. As can be seen, the transmittance increases as the ITO film etching time increases, except at the 500 nm wavelength. At most of the wavelengths, the transmittance increases by approximately 10%. The SEM images and transmission spectroscopy results show that the increase in transmittance can be attributed to the formation of the ITO nanorod layer. In the ITO nanorod layer, ITO mixes with air or hole transporting material, thus resulting in a gradient refractive index, which is essential for an antireflection layer.[23,24] Moreover, the dark-field microscopy image of the ITO nanorod layer (Figure 3b) is brighter than that of the ITO film (Figure 3c). Because a dark-field microscope can collect only scattered light, the brighter image of the ITO nanorod layer, when compared with that of the ITO film, indicates the stronger light-scattering behavior of the ITO nanorod layer.

Because the ITO nanorod layer possesses excellent optical characteristics, such as high transmittance and strong light-scattering behavior, output coupling of light can be enhanced in LEDs. Therefore, the ITO nanorod layer was embedded in a PLED to demonstrate its merits. To fabricate the PLEDs, we used PEDOT:PSS as the hole-transporting layer on the ITO nanorods, and a blend film consisting of poly(*N*-vinyl

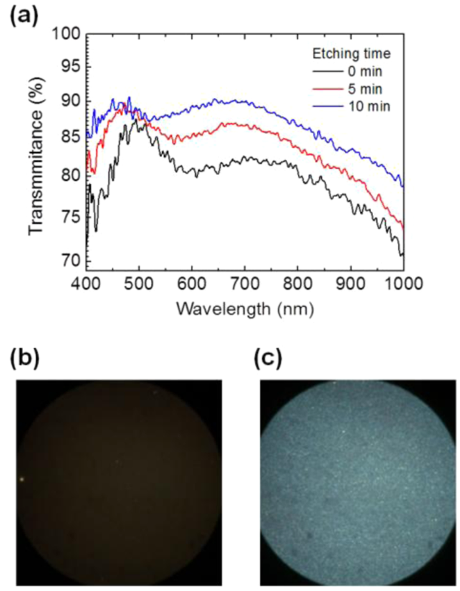

Figure 3. (a) Transmittance spectra of ITO layer etched for different periods of time. Dark-field microscope images of (b) ITO film and (c) ITO nanorods etched for 10 min.

carbazole) (PVK), 2-(4-*tert*-Butylphenyl)-5-(4-biphenylyl)-1,3,4-oxadiazole (PBD), N,N′-bis(3-methylphenyl)-N,N′-diphenylbenzidine (TPD), and tris(2-(4-tolyl)phenylpyridine) iridium ($Ir(mppy)_3$) was used as the emissive layer. Further, LiF and Al were used as the cathode (Figure 1). The device structure is glass substrate/ITO nanorods/PEDOT:PSS/PVK:PBD:TPD:$Ir(mppy)_3$/LiF/Al. Green phosphorescent dopant $Ir(mppy)_3$ was blended with PVK host polymer. Further, TPD and PBD were also blended with PVK to facilitate hole and electron transport, respectively, because of the high hole mobility of TPD ($\mu_h \approx 1 \times 10^{-3}$ cm^2 V^{-1} s^{-1})[25] and the high electron mobility of PBD ($\mu_e \approx 1 \times 10^{-5}$ cm^2 V^{-1} s^{-1}).[26] The commonly used weight blending ratio of PVK:PBD:TPD:$Ir(mppy)_3$ = 61:24:9:6[27,28] was selected. However, the wetting properties of PEDOT:PSS on ITO nanorods are poor, and the gaps between the ITO nanorods were not completely filled with PEDOT:PSS after spin coating. Therefore, the PEDOT:PSS was blended with isopropanol and Triton X-100 to improve the wetting properties of PEDOT:PSS on ITO nanorods. As shown in Figure 4a, after the wetting problem is resolved by adding additives to the PEDOT:PSS, the gaps between the ITO nanorods are filled. The thickness of PEDOT above the ITO nanorods is approximately 20 nm. The device fabrication process was completed by further depositing an emissive layer of approximately 100 nm and LiF/Al as the cathode, as shown in Figure 4c. A reference device with an ITO film as the transparent anode was also fabricated, as shown in Figure 4b, d. The thickness of each layer was controlled to ensure that the layers are comparable to those of the device with the ITO nanorod layer.

The characteristics of the device embedded with ITO nanorods were analyzed and compared with those of the reference device without ITO nanorods, as shown in Figures 5a, b. The maximum current efficiency of the reference device without ITO nanorods is 2.86 cd/A whereas it is 5.47 cd/A for the device with ITO nanorods. The superior current efficiency of the device with ITO nanorods can be attributed to the

DOI: 10.1021/acsami.5b01117
ACS Appl. Mater. Interfaces 2015, 7, 7462−7465

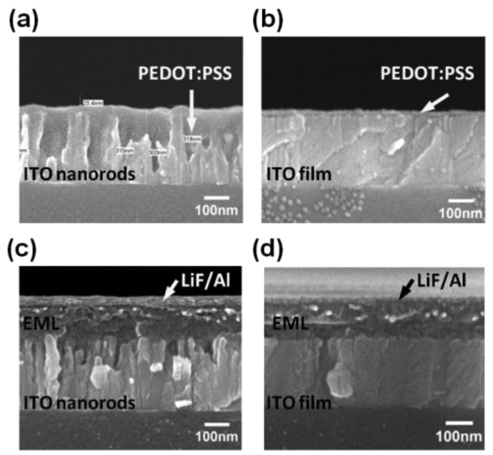

Figure 4. SEM images of PEDOT:PSS layer on (a) ITO nanorod layer and (b) ITO film. SEM images of devices (c) with and (d) without ITO nanorod layer.

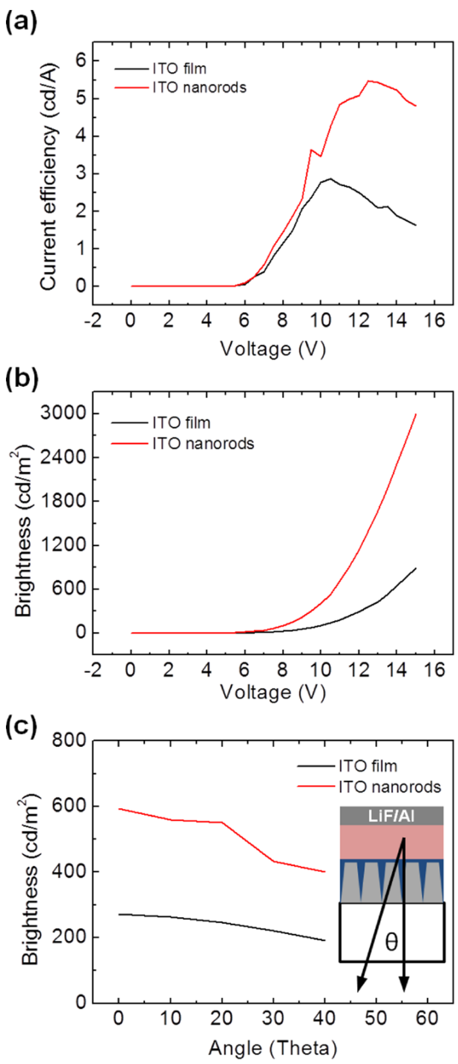

Figure 5. (a) Current efficiency and (b) brightness of polymer light-emitting diodes with and without ITO nanorods. (c) Variation in brightness with viewing angle.

greater brightness (Figure 5b). The high transmittance of the ITO nanorod layer significantly influences the brightness; hence, the light out-coupling and current efficiencies are enhanced. Moreover, the current density values at 11 V are 6.68 and 14.64 mA/cm^2 for the devices without and with ITO nanorods, respectively. The higher efficiency for the device with ITO nanorods can also be attributed to the higher current density. The higher current density is the result of a rougher interface between the electrode and the emissive layer, which promotes charge injection (Figure 4a).

The angular dependency of brightness was also analyzed. The brightness at different viewing angles (θ) was recorded, as shown in Figure 5c. The brightness of the device with ITO nanorods is greater than that of the device without nanorods at different viewing angles because of the light-scattering nature of the ITO nanorods. Therefore, more light is out-coupled at different angles. A device with enhanced performance can be achieved by using ITO nanorods, which can be fabricated in only 10 min.

In summary, PLEDs embedded with ITO nanorods were realized. The ITO nanorods were fabricated in 10 min using wet chemical etching method and embedded in PLEDs for light extraction. The brightness and current efficiency of the PLED with ITO nanorods were enhanced. This enhancement in efficiency can be attributed to the excellent optical characteristics such as high transmittance and stronger light-scattering characteristics of the ITO nanorods.

■ ASSOCIATED CONTENT

Supporting Information

Details of experimental procedures. This material is available free of charge via the Internet at http://pubs.acs.org.

■ AUTHOR INFORMATION

Corresponding Author

* E-mail: ycchao@cycu.edu.tw.

Notes

The authors declare no competing financial interest.

■ ACKNOWLEDGMENTS

This work was supported by the Ministry of Science and Technology of Taiwan under Grants MOST103-2633-M-033-004 and MOST103-2112-M-033-005-MY3.

■ REFERENCES

(1) Shen, H.; Bienstman, P.; Maes, B. Plasmonic Absorption Enhancement in Organic Solar Cells with Thin Active Layers. *J. Appl. Phys.* **2009**, *106*, 073109.

(2) Moulé, A. J.; Bonekamp, J. B.; Meerholz, K. The Effect of Active Layer Thickness and Composition on the Performance of Bulkheterojunction Solar Cells. *J. Appl. Phys.* **2006**, *100*, 094503.

(3) Lee, W. H.; Chen, H. L.; Chuang, S. Y.; Chen, T. H.; Su, W. F. Using Optical Thin Film Model to Optimize Thermal Annealing Procedure in P3HT:PCBM Blend Based Solar Cells. *Proc. SPIE* **2008**, *6999*, 69991L.

(4) Luo, Y.; Wang, L.; Ding, Y.; Li, L.; Shi, J. High Light-Extracting Efficiency for OLED Directly Fabricated on Double-Side Nanotextured Silica Substrate. *Opt. Lett.* **2013**, *38*, 2394−2396.

(5) Hong, K.; Lee, J. L. Review Paper: Recent Developments in Light Extraction Technologies of Organic Light Emitting Diodes. *Electron. Mater. Lett.* **2011**, *7*, 77−91.

(6) Reboud, V.; Khokhar, A. Z.; Sepúlveda, B.; Dudek, D.; Kehoe, T.; Cuffe, J.; Kehagias, N.; Lira-Cantu, M.; Gadegaard, N.; Grasso, V.; Lambertini, V.; Torres, C. M. S. Enhanced Light Extraction in ITO-Free OLEDs Using Double-Sided Printed Electrodes. *Nanoscale* **2012**, *4*, 3495.

DOI: 10.1021/acsami.5b01117
ACS Appl. Mater. Interfaces 2015, 7, 7462−7465

(7) Madigan, C. F.; Lu, M. H.; Sturm, J. C. Improvement of Output Coupling Efficiency of Organic Light-Emitting Diodes by Backside Substrate Modification. *Appl. Phys. Lett.* **2000**, *76*, 1650−1652.
(8) Wu, C. C.; Wu, C. I.; Sturm, J. C.; Kahn, A. Surface Modification of Indium Tin Oxide by Plasma Treatment: An Effective Method to Improve the Efficiency, Brightness, and Reliability of Organic Light Emitting Devices. *Appl. Phys. Lett.* **1997**, *70*, 1348−1350.
(9) Gu, G.; Garbuzov, D. Z.; Burrows, P. E.; Venkatesh, S.; Forrest, S. R.; Thompson, M. E. High-External-Quantum-Efficiency Organic Light-Emitting Devices. *Opt. Lett.* **1997**, *22*, 396−398.
(10) Nakamura, T.; Tsutsumi, N.; Juni, N.; Fujii, H. Thin-Film Waveguiding Mode Light Extraction in Organic Electroluminescent Device Using High Refractive Index Substrate. *J. Appl. Phys.* **2005**, *97*, 054505.
(11) Möller, S.; Forrest, S. R. Improved Light Out-Coupling in Organic Light Emitting Diodes Employing Ordered Microlens Arrays. *J. Appl. Phys.* **2002**, *91*, 3324−3327.
(12) Wei, M. K.; Su, I. L. Method to Evaluate the Enhancement of Luminance Efficiency in Planar OLED Light Emitting Devices for Microlens Array. *Opt. Express* **2004**, *12*, 5777−5782.
(13) Do, Y. R.; Kim, Y. C.; Song, Y. W.; Lee, Y. H. Enhanced Light Extraction Efficiency from Organic Light Emitting Diodes by Insertion of a Two-Dimensional Photonic Crystal Structure. *J. Appl. Phys.* **2004**, *96*, 7629−7636.
(14) Liu, C.; Kamaev, V.; Vardeny, Z. V. Efficiency Enhancement of an Organic Light-Emitting Diode with A Cathode Forming Two-Dimensional Periodic Hole Array. *Appl. Phys. Lett.* **2005**, *86*, 143501.
(15) Lee, Y. J.; Kim, S. H.; Huh, J.; Kim, G. H.; Lee, Y. H.; Cho, S. H.; Kim, Y. C.; Do, Y. R. A High-Extraction-Efficiency Nanopatterned Organic Light-Emitting Diode. *Appl. Phys. Lett.* **2003**, *82*, 3779−3781.
(16) Tsutsui, T.; Takada, N.; Saito, S.; Ogino, E. Sharply Directed Emission in Organic Electroluminescent Diodes with an Optical-Microcavity Structure. *Appl. Phys. Lett.* **1994**, *65*, 1868−1870.
(17) Bulović, V.; Khalfin, V. B.; Gu, G.; Burrows, P. E.; Garbuzov, D. Z.; Forrest, S. R. Weak Microcavity Effects in Organic Light-Emitting Devices. *Phys. Rev. B* **1998**, *58*, 3730−3740.
(18) Chiu, N. F.; Lin, C. W.; Lee, J. H.; Kuan, C. H.; Wu, K. C.; Lee, C. K. Enhanced Luminescence of Organic/Metal Nanostructure for Grating Coupler Active Long-Range Surface Plasmonic Device. *Appl. Phys. Lett.* **2007**, *91*, 083114.
(19) Zheng, T.; Choy, W. C. H.; Sun, Y. Nanoparticle-Induced Resonant Tunneling Behaviors in Small Molecule Organic Light-Emitting Devices. *Appl. Phys. Lett.* **2009**, *94*, 123303.
(20) Nien, S. Y.; Chiu, N. F.; Ho, Y. H.; Lee, J. H.; Lin, C. W.; Wu, K. C.; Lee, C. K.; Lin, J. R.; Wei, M. K.; Chiu, T. L. Directional Photoluminescence Enhancement of Organic Emitters via Surface Plasmon Coupling. *Appl. Phys. Lett.* **2009**, *94*, 103304.
(21) Chao, Y. C.; Zhan, F. M.; Li, H. D. Indium-Tin-Oxide Nanorods for Efficient Light Trapping in Polymer Solar Cells. *RSC Adv.* **2014**, *4*, 30881−30886.
(22) Chiu, C. H.; Yu, P.; Chang, C. H.; Yang, C. S.; Hsu, M. H.; Kuo, H. C.; Tsai, M. A. Oblique Electron-Beam Evaporation of Distinctive Indium-Tin-Oxide Nanorods for Enhanced Light Extraction from InGaN/GaN Light Emitting Diodes. *Opt. Express* **2009**, *17*, 21250−21256.
(23) Chattopadhyay, S.; Huang, Y. F.; Jen, Y. J.; Ganguly, A.; Chen, K. H.; Chen, L. C. Anti-Reflecting and Photonic Nanostructures. *Mater. Sci. Eng. R-Rep.* **2010**, *69*, 1−35.
(24) Raut, H. K.; Ganesh, V. A.; Nair, A. S.; Ramakrishna, S. Anti-Reflective Coatings: A Critical, In-Depth Review. *Energy Environ. Sci.* **2011**, *4*, 3779−3804.
(25) Kuwahara, A.; Naka, S.; Okada, H.; Onnagawa, H. Carrier Mobility of Organic Thin Films Using Lateral Electrode Structure with Optical Slits. *Appl. Phys. Lett.* **2006**, *89*, 132106.
(26) Kawabe, Y.; Abe, J. Electron Mobility Measurement Using Exciplex-Type Organic Light-Emitting Diodes. *Appl. Phys. Lett.* **2002**, *81*, 493−495.
(27) Cai, M.; Xiao, T.; Hellerich, E.; Chen, Y.; Shinar, R.; Shinar, J. High-Efficiency Solution-Processed Small Molecule Electrophosphorescent Organic Light-Emitting Diodes. *Adv. Mater.* **2011**, *23*, 3590−3596.
(28) Cai, M.; Xiao, T.; Chen, Y.; Hellerich, E.; Liu, R.; Shinar, R.; Shinar, J. Effect of Molecular Weight on the Efficiency of Poly(N-vinylcarbazole)-Based Polymer Light-Emitting Diodes. *Appl. Phys. Lett.* **2011**, *99*, 203302.

DOI: 10.1021/acsami.5b01117
ACS Appl. Mater. Interfaces 2015, 7, 7462−7465